PERFORMANCE OF MOLTEN SALT SODIUM/β-ALUMINA/SbCl₃ CELLS*

A. M. CHREITZBERG, J. W. CONSOLLOY, M. R. MANNING and J. C. SKLARCHUK

ESB Technology Company, Technology Center, 19 W. College Avenue, Yardley, Pennsylvania 19067 (U.S.A.)

Summary

Twenty watt-hour size cells were tested at 180° - 260 °C to observe performance trends as a function of charge and discharge rate, temperature and cycling on a 3 cycle per day routine. Major components of the test geometry were a carbon steel outer sodium container, a beta alumina separator tube 2.5 cm o.d. × 15 cm long × 2 mm wall thickness, spiral nickel or molybdenum brush current collectors, and a positive mix of carbon powder, sodium chloroaluminate and antimony trichloride.

Energy input and output, energy efficiency and antimony utilization were monitored at discharge rates of 3, 5, 7, 10 and 14 hours and charge rates of 3, 5, 7 and 10 hours to 100% depth (4.0 V top of charge and 1.9 V bottom of discharge).

Scaled up 50 and 80 Wh cells were constructed and tested. Projections of the performance of 200 Wh cells and the cost of a 100 MWh battery are given for utility load leveling applications.

Introduction

Sodium–antimony trichloride cells have been in development by ESB Ray-O-Vac Corporation as a moderate temperature molten salt energy storage system since 1970. Cell designs are directed at specifications for utility load leveling and fork lift truck battery applications. Summary reports have been published by the Electric Power Research Institute describing chemical compatibility tests, beta alumina development and cathode composition optimization tests conducted in the period 1974 - 1977 [1, 2]. This report will focus on life cycle tests of early 20 Wh single tube cells, current collector design, first scale-up cells and a price projection of a 100 MWh load leveling battery.

Electrochemistry of the molten salt cell

The cell reaction in its simplest form is:

$$3Na + SbCl_3 \underset{C}{\overset{D}{\rightleftharpoons}} \underline{Sb} + \underline{NaCl}$$
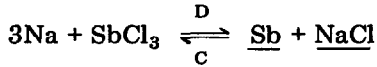
Non-conducting $SbCl_3$ is dissolved in a mixture of NaCl and $AlCl_3$ which react to form Na^+, $AlCl_4^-$, the conductive salt in the cathode compartment. Sodium chloride produced on discharge reacts with excess $AlCl_3$ in the melt forming soluble, conductive sodium tetrachloroaluminate. The operating temperature range of 180 - 240 °C is limited by the melt composition, the insolubility of uncomplexed NaCl at the bottom-of-discharge and the vapor pressure of free $AlCl_3$ and $SbCl_3$ at the top-of-charge. Figure 1 gives the controlling phase diagram and the operating range of present cells.
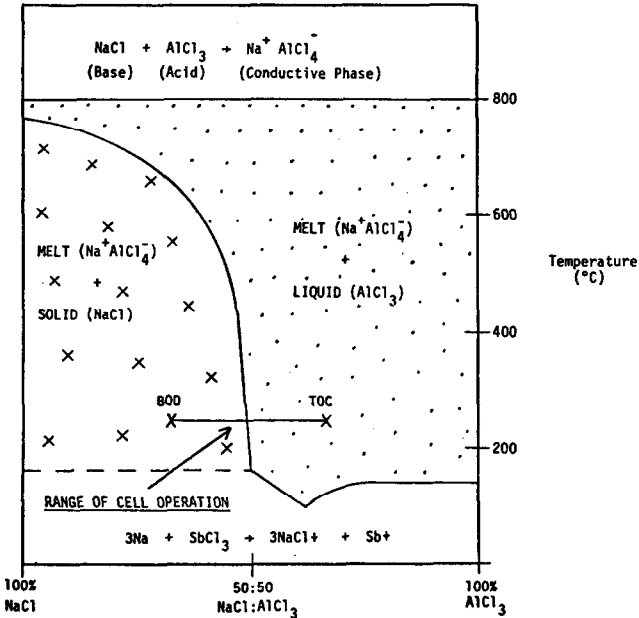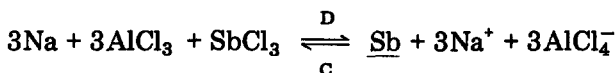

Fig. 1. Phase diagram of NaCl–AlCl₃ melt.

To maintain maximum NaCl solubility and freedom from polarization at the bottom-of-discharge the reaction can be represented by the equation:

$$3Na + 3AlCl_3 + SbCl_3 \underset{C}{\overset{D}{\rightleftharpoons}} \underline{Sb} + 3Na^+ + 3AlCl_4^-$$

Some excess of $NaAlCl_4$ must also be available at the top-of-charge to provide chloride ion for the charge reaction and a conductive mix to prevent severe polarization. Present positive mixes contain about 29%
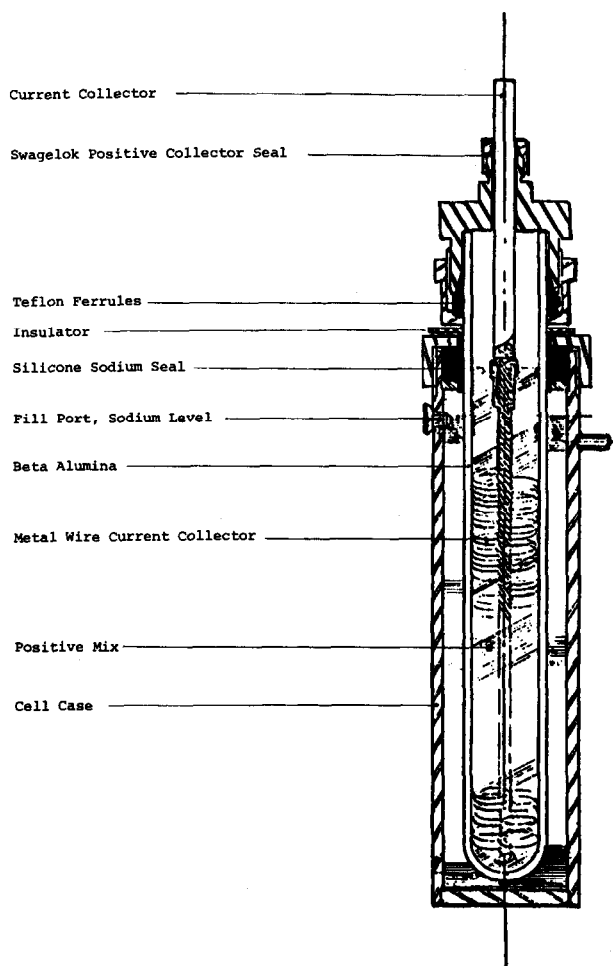
Current Collector ———————————

Swagelok Positive Collector Seal ——————

Teflon Ferrules ————————————

Insulator ——————————

Silicone Sodium Seal ———————

Fill Port, Sodium Level ———————

Beta Alumina ——————————

Metal Wire Current Collector ——————

Positive Mix ——————————

Cell Case ——————————

Fig. 2. Twenty watt-hour test cell.

$SbCl_3$ by weight and are selected to give maximum energy output at specified rates while delivering competitive cycle life.

Description of test cells

Figure 2 is a sketch of the 20 Wh size test cell. The positive $SbCl_3$–salt melt is inside a beta alumina tube having the dimensions of 2.5 cm o.d. × 15 cm long × 2 mm in wall thickness. Sodium in the molten state is outside the beta-alumina tube and contained in a carbon steel cell case sealed by a silicone gasket to the tube. The positive compartment is sealed by a Swagelok compression seal having a positive terminal crimped to a metal wire current collector. The 20 Wh 10-hour rating is the upper limit of energy

output for 67 g positive mix and a mix height inside the tube of 10 cm, or 36 cm^3 of mix.

Beta alumina tubes were fabricated by the ESB Ceramic Laboratory and the compositions were nominally 8.0% Na_2O, 2.0% MgO and 90% Al_2O_3. Average properties were: (1) specific resistivity 25 ± 10 ohm-cm at 200 °C; (2) diametral break strength 700 - 1100 kg/cm^2; and (3) a density of 3.14 - 3.20 g/cm^3. Lithia-doped β'' alumina tubes were also fabricated lowering the specific resistivity to 10 ± 5 ohm-cm at 200 °C and increasing the break strength to 1260 - 1330 kg/cm^2. Lithia-doped β'' alumina had a nominal composition of 0.7% Li_2O, 8.7% Na_2O and 90.6% Al_2O_3. The best Na/Na test life was 1800 Ah/cm^2 achieved by β'' alumina tubes 2.5 cm o.d. × 15 cm × 2 mm at a current density of 0.56 A/cm^2 accumulated in the discharge direction.

A series of 20 Wh-size cells was constructed to test the relative merits of molybdenum spiral current collectors having differing weights, surface areas and conductivity and the cycle life of magnesia-doped beta-alumina tubes. Molybdenum and tungsten were optional choices for the collector metal; however, only molybdenum could be readily fabricated into the spiral designs and was also more economical.

Each cell had a theoretical antimony capacity of 6.84 Ah and the only design variable was the positive mix collector area and weight.

Cell	Spiral wire		Stem wire diameter (cm)	Total collector	
	Diameter (cm)	Length (m)		Weight (g)	Area (cm^2)
A	0.013	22.4	0.076	5.78	94
B	0.020	11.2	0.076	6.38	76
C	0.013	11.2	0.076	4.40	49
D	0.013	11.2	0.051	3.36	48

A similar 20 Wh cell was assembled with a carbonized nickel current collector fabricated from two twisted 0.11 cm diameter stem wires and 0.015 cm diameter spiral wire to give an area of 134 cm^2 and a weight of 14.0 g. Carbonization of the nickel surface left a conductive carbon film with an actual surface, confirmed by capacitance measurements, of 8 - 10 times the calculated surface.

These five cells were cycled at 210 ± 10 °C in helium atmosphere boxes as follows: (1) forming 10 h rate cycles to steady state capacities, then an initial discharge rate study with successive 100% depth discharges at the 14, 10, 7, 5 and 3 h rate holding a constant 14 h rate charge to a 4.0 V cut-off; (2) initial charge rate study with successive charges at the 14, 10, 7, 5 and 3 h rate while holding the discharge rate constant at the 10 h rate; then

(3) cycling 3 cycles per day on a 3 h discharge/5 h charge routine between the voltage limits of 4.0 V top-of-charge and 1.9 V discharge cut-off; (4) after about 250 cycles (1) and (2) were repeated, and cycling was continued as in (3) to failure of the first two cells in the group.

One objective was to scale-up to a production 200 Wh size cell using a single ceramic tube 4.5 cm o.d. × 43 cm long × 2 - 3 mm wall thickness. A first step was completed with a scale-up from 20 Wh to 80 Wh using lithia-doped β'' alumina tubes 4.4 cm o.d. × 17 cm long × 2 mm walls.

The first two cells incorporated improved silicone anode seals, with initial sealing compression controlled to 70 kg/cm^2, and Swagelok positive seals having Teflon ferrules compressed directly upon the beta alumina tube. Theoretical discharge capacities were 19.9 and 29.1 Ah for positive mix weights of 212 and 310 grams respectively. At average open circuit voltages of 2.75 V the maximum cell energy outputs were projected to be 55 and 80 Wh.

The current collectors were straight molybdenum wire type having the following features:

Cell design		Collector design	
Energy (Wh)	Stem wire No., diam., and length (cm)	Straight wire No., diam., and length (cm)	Active area (cm^2)
55	2 × 0.152 × 20	4.0 × 0.020 × 540	135
80	2 × 0.076 × 20	4.0 × 0.013 × 1108	181

Each cell was made in the discharged state with a positive mix composition having 34.3% NaCl, 43.6% AlCl$_3$, 14.2% Sb powder, 6.7% carbon black and 1.2% by weight sulfur. At 200 °C the density of the mix was 1.95 g/cm^3.

The cells were formation charged at the 16 h rate and cycled at 210 °C until capacity leveled, then discharge and charge rate tests were performed.

Cycle test results

Table 1 summarizes the relative performance of the 20 Wh cells as a function of the current collector design. Figure 3 plots the voltages of cell type A *versus* discharge capacity at the 10, 7 and 5 h rates after charge at the 14 h rate — all observed between cycle 10 and 20. Figure 4 plots the similar data after 130 deep cycles. Coulombic inefficiency was noticed first during the delayed charge rate study, and cell testing had to be terminated after 244 cycles because of a cracked beta alumina tube.

Polarization of cell type A is shown in Fig. 5 as the difference between the equilibrium open circuit voltage in its steady state and the loaded voltage

TABLE 1

Effect of positive current collector design on energy output on rate tests before and after cycling

Design or performance parameter	Unit	Cell type			
		A	B	C	D
Collector area	cm^2	94	76	50	48
Collector weight	g	5.8	6.4	4.4	3.4
Stem diameter	cm	0.051	0.076	0.076	0.076
Time on test	h	4008	5056	4911	4935
Cycles between rate tests	ea	130	250	260	260
Cycles on test (total)	ea	244	450	502	499
Mean capacity first 150 cycles	Ah	5.7	5.4	4.5	4.1
Utilization (Sb)	%	83	79	66	60
Accumulative capacity to test end[3]	Ah/cm^2 β alumina	44	50	54	32
Energy output					
before cycling	Wh	Wh	Wh	Wh	Wh
loss after cycling	(%)	(%)	(%)	(%)	(%)
Discharge rate[1]					
0.5 A		17.5(5)	17.7(26)	16.4(24)	16.3(43)
1.0 A		16.3(8)	17.2(34)	14.5(28)	14.2(46)
2.4 A		13.0(13)	14.9(33)	10.3(20)	10.0(51)
4.8 A		10.4(25)	—	—	—
Charge rate[2]					
0.5 A		19.8(13)	19.7(27)	16.6(20)	16.5(20)
1.0 A		19.3(15)	19.4(32)	16.1(30)	14.5(24)
2.4 A		18.7(24)	15.0(24)	7.9(—)	5.6(—)
Turnaround energy efficiency	%				
Discharge rate[1]					
0.5 A		88	90	91	86
1.0 A		86	87	83	82
2.4 A		71	77	74	60
Failure mode		Beta cracked	Seal	VT	VT

[1] Charge rate held constant at 14 h.
[2] Discharge rate held constant at 10 h.
[3] Sum of charge and discharge capacity.

at the 5 and 10-hour charge and discharge rates. Polarization tends to increase with increasing state-of-charge. Figure 4 gives evidence that polarization also increases with cycle life when its voltages are compared with those of Fig. 3.

Cell type B, with a collector having 18% less surface area and 9% heavier spiral wire, performed competitively with cell type A initially, and output energy loss measured after 250 cycles was more than twice as great
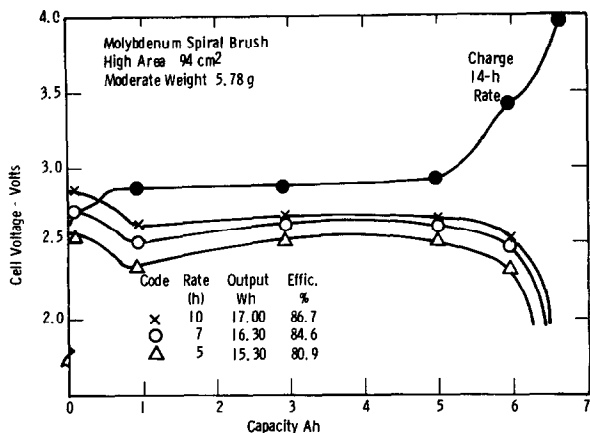
Molybdenum Spiral Brush
High Area 94 cm²
Moderate Weight 5.78 g

Charge
14-h
Rate

Code	Rate (h)	Output Wh	Effic. %
×	10	17.00	86.7
○	7	16.30	84.6
△	5	15.30	80.9

Fig. 3. Voltage *vs.* discharge capacity for cell A rate tests before cycling.

Molybdenum Spiral Brush
High Area 94 cm²
Moderate Weight 5.78 g

Charge
14-h Rate

Code	h	Wh	Effic. (%)
×	10	16.0	89.5
○	7	15.0	86.1
△	5	13.8	80.2
□	3	11.4	71.2
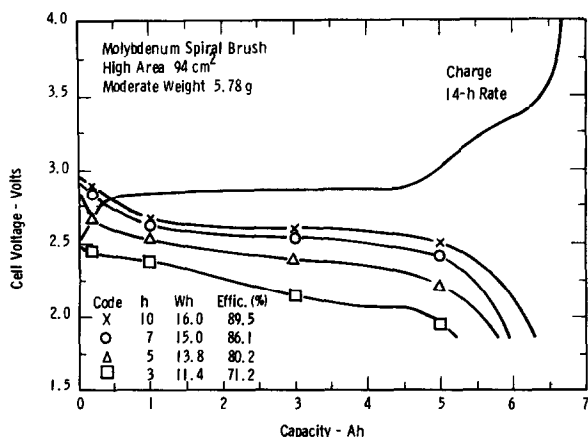
Fig. 4. Voltage *vs.* discharge capacity for cell A after 130 cycles.

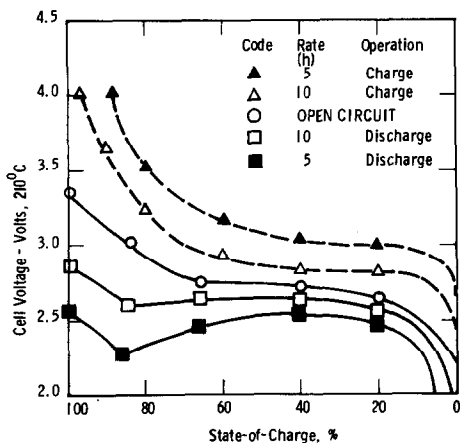| Code	Rate (h)	Operation
▲	5	Charge
△	10	Charge
○	OPEN CIRCUIT	
□	10	Discharge
■	5	Discharge

Fig. 5. Charge and discharge loaded voltages and open circuit voltage *vs.* state-of-charge for Na/β-alumina/NaAlCl$_4$, SbCl$_3$ system.

as cell type A measured after 130 cycles. Figure 6 gives the discharge rate study curves after 250 deep cycles on the 3 cycle per day routine. Testing was terminated after 450 cycles. Capacity decay could have been accelerated by the positive seal leak which was the ultimate mode of failure. Figure 7 gives the capacity *versus* cycle life history. Repeated topping-off charges to 4.0 V were required to maintain capacity.
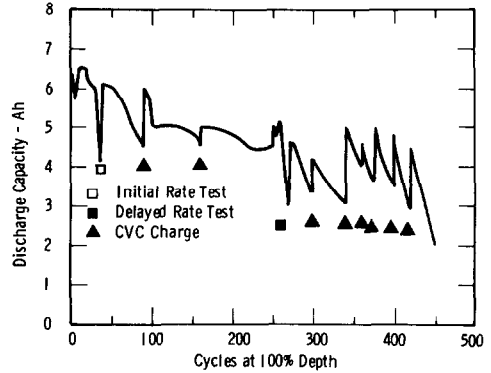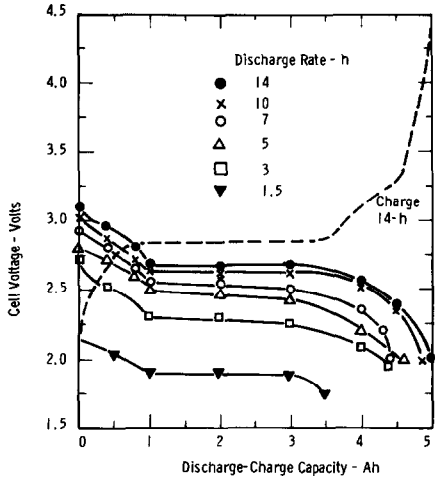

Fig. 6. Voltage *vs.* discharge capacity for cell B after 250 cycles.

Fig. 7. Cycle history of cell B with high weight–moderate area Mo collector.

Cells type C and D, while delivering less energy per cycle, operated without failure for 500 deep cycles. Their current collectors had only 48% of the surface area and 76 and 59% of the weight respectively of the collector type A. Energy output at higher charge and discharge rates was also much less than that of cell type A.

In most electrochemical systems a charge process which involves oxidation of a conductive metal to a non-conductive metal compound limits the capacity delivered. The charge process of the Na/SbCl$_3$ system also limits output capacity. Figure 8 gives log current *versus* log time plots for cell type A with the best performing high area collector (top curves) and for type D with the worst performing low area current collector. In both cells the charge current *vs.* charge time curves depart from linearity first, showing that the charge process and the charge current density in amperes per unit area of collector limit charge input, and therefore discharge output capacity.

Figure 9 gives the cycle history of the cell with a carbonized nickel current collector. During 100 deep cycles on the 3-cycle per day routine output was remarkably constant, and weekly topping-off charges were not needed as experienced with molybdenum collector cells. Antimony utilization and turnaround energy efficiency were maintained at attractively high levels and to cycle 108 where coulombic inefficiency appeared. Testing was terminated at cycle 129.
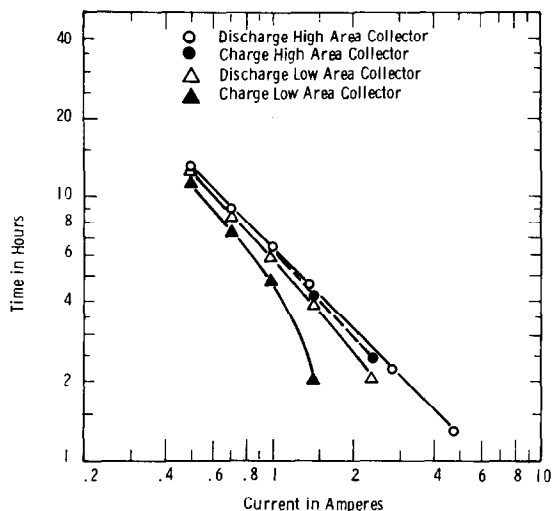
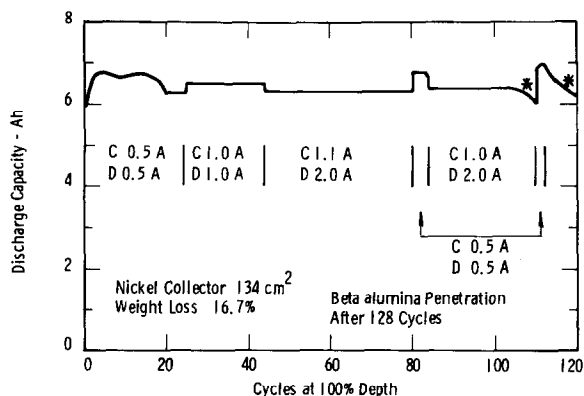Fig. 8. Log charge (or discharge) current *vs.* log time for cell types A and D.

Fig. 9. Cycle history of cell with carbonized nickel brush collector.

TABLE 2

Discharge rate tests on 55 Wh cell

Nominal rate (h)	Discharge[1,2]		Mean cell voltage		Energy output (Wh)	Utilization (%)	Energy efficiency (%)
	Current (A)	Capacity (Ah)	Discharge (V)	Charge (V)			
16	1.25	20.2	2.66	2.95	53.8	97	90
10	2.00	19.8	2.57	2.98	50.8	95	86
7	2.85	19.4	2.47	2.96	48.0	93	83
5	4.00	19.0	2.34	2.97	44.4	91	79
3	6.67	18.2	2.14	2.93	39.0	87	73
1	10.00	12.9	1.89	—	24.4	62	—

[1]Recharge rate held constant at 1.25 A to 4.00 V.
[2]Discharge to 1.9 V or knee of curve.

TABLE 3

Discharge rate tests on 80 Wh cell

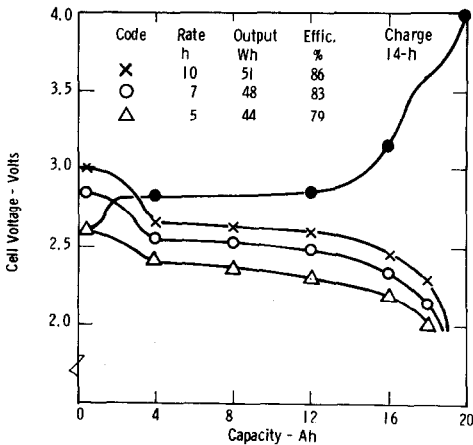| Nominal rate (h)	Discharge[1,2]		Mean cell voltage		Energy output (Wh)	Utilization (%)	Energy efficiency (%)
	Current (A)	Capacity (Ah)	Discharge (V)	Charge (V)			
14	2.00	28.4	2.63	3.02	74.8	93	87
10	2.86	28.3	2.51	3.02	71.1	93	83
7	4.00	26.4	2.42	2.97	63.9	86	81
5	5.60	24.1	2.32	2.96	55.8	79	78
2	9.50	18.3	2.16	2.99	39.5	60	72

[1] Recharge rate held constant at 2.00 A to 4.00 V.
[2] Discharge to 1.9 V or knee of curve.

Fig. 10. Voltage *vs.* discharge capacity of 55 Wh cell.

The 55 and 80 Wh cells were tested in a charge–discharge rate study in the same manner as the 20 Wh cells. Table 2 is a summary of discharge energy output, antimony utilization and energy efficiency for the 55 Wh cell when discharged at the nominal 16, 10, 7, 5, 3 and 1 h rates and recharged always at the 16 h rate to 4.0 V. Table 3 is similar data for the 80 Wh cell. Figures 10 and 11 give voltage *versus* discharge capacity plots for the 10, 7 and 5 h rates for each cell. The greater conductivity in the stem and straight bristles of the collector in the 55 Wh cell produced greater specific output than the output of the 80 Wh cell. Table 4 shows the relative loss in performance when the beta alumina tube diameter is increased from 2.5 cm to 4.4 cm and the positive active mix volume is increased from 34 to 159 cm^3. This loss must in great part be compensated for by heavier and more conductive collector stems, by changes in collector wire array and by changes in positive mix composition.
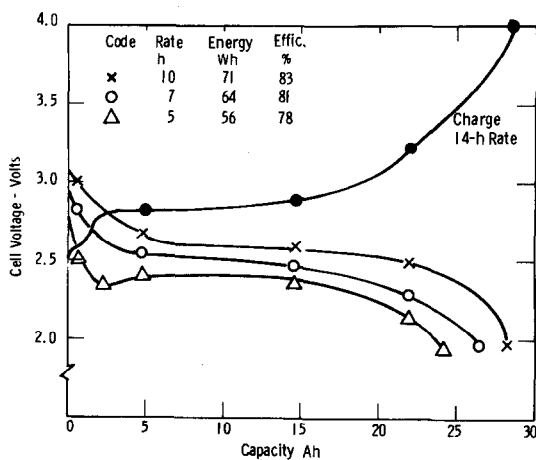
Fig. 11. Voltage *vs.* discharge capacity for 80 Wh cell.

TABLE 4

Effect of tube diameter and length on cell energy output

Cell size (Wh)	Tube dimensions (cm)		Active mix (cm³)	Energy output[1] (Wh/cm³)	
	Diameter	Length (active)		10 h	5 h
20	2.5	10	34	0.51	0.48
55	4.4	9	109	0.47	0.41
80	4.4	12	159	0.45	0.35

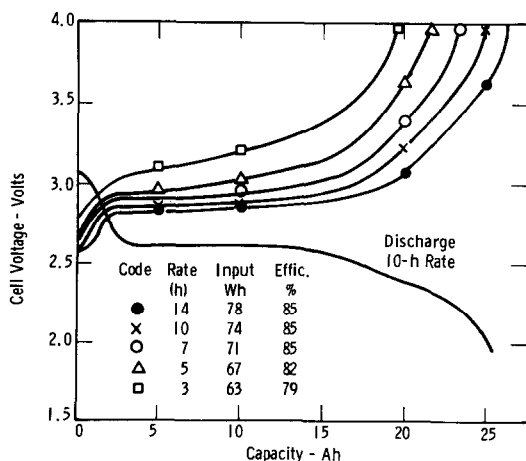[1] Energy per unit volume of positive mix.

Fig. 12. Voltage *vs.* charge capacity for 80 Wh cell.

Figure 12 gives the decrease in charge input at increasing charge rates for the 80 Wh cell and the resulting decrease in energy efficiency measured by a 10 h rate discharge.

Cell dissection and failure analysis

Cells C and D were dissected on the same day. While both cells delivered 500 cycles, each would have failed earlier had the tests not been performed in a helium atmosphere. The anode silicone seals had failed from cracking embrittlement exposing the sodium to the helium box atmosphere.

The bottom 1/3 of the beta alumina tubes remained well wetted with Na. The middle 1/3 was partly wetted with Na and covered with a yellowish froth which also was floating on the Na surface. This partial dewetting of the beta alumina tubes below the normal Na level is associated with anode seal failure and is clearly one mechanism of capacity loss during cycling.

Cell A failed prematurely by a circumferential crack near the bottom of its beta alumina tube and subsequent sodium short to the positive mix. Cell B failed by a positive Teflon seal leak which allowed escape of volatile $SbCl_3$ and a cathode capacity loss.

The positive active mix was washed away from the molybdenum brushes on cells C and D, and the loss in weight of the collector was taken as a measure of corrosion during the 500 cycle test at 200 - 220 °C. Weight losses ranged from 29 to 40%. This corrosion of molybdenum under the accelerated test conditions influenced cell output on the lightweight collectors more than on the heavy collectors; however, its magnitude eliminates Mo from further consideration as a long life current collector.

Failure analysis of the cell with a carbonized nickel collector revealed penetration of the beta-alumina tube partly by sodium from the outside and an aluminum deposit from the inside. The nickel collector was corroded extensively losing 16.5% by weight or 22 mg/cm^2 in the 50 day test at 210 °C.

Performance projections of larger cells and module price estimate

Scale-up to 100 and 200 Wh size cells are projected with changes in positive mix composition and current collector design to reach an energy output goal of 0.41 Wh/cm^3 of positive mix. Table 5 gives the projected dimensions of these single tube cells and estimates of their performance at 10, 7 and 5 h rates.

Using this standardized costing method proposed by the Arthur D. Little study, an estimate of the price of 100 MWh battery modules has been made and is given in Table 6 [3]. In a dedicated single product plant, an estimated price of $39/kWh is projected at a production rate of 2500 MWh per year.

Future developments and problem areas

Fundamental electrochemical investigations of corrosion of the metal current collector are in progress. Pure nickel electrodes corrode at acceptable

TABLE 5

100 and 200 Wh size cell performance projection

Design-performance parameter	Unit	100 Wh cell	200 Wh cell
Dimensions: o.d.	cm	5.3	5.3
length	cm	26	51
Volume	litres	0.57	1.13
Weight	kg	1.26	2.33
Capacity, rated	Ah	35	80
Energy output to 2.0 V			
Discharge rate:	Wh		
10 h		99	220
7 h		96	215
5 h		92	205
Energy density to 2.0 V			
Discharge rate:			
10 h	Wh/l	174	195
5 h		161	181
10 h	Wh/kg	79	94
5 h		73	88

TABLE 6

100 MWh battery modules price estimate

Cost element	$MM	$/kWh	%
Positive and negative materials	13.25	5.31	13.4
Cell, tray, connector hardware	15.46	6.18	15.6
Positive current collector	11.71	4.68	11.8
Beta alumina tube and alpha cap	7.45	2.98	7.5
Total material and purchased parts	47.87	19.15	48.3
Material overheads at 10%	4.79	1.92	4.8
Direct labor at $7.50/h	12.99	5.20	13.1
(beta alumina, cell assembly, processing)			
Overheads at 150%	19.49	7.79	19.8
Equipment depreciation (10 year)	1.44	0.57	1.4
Rental at $3.75/ft^2	0.28	0.11	0.3
Factory cost (FC):	86.86	34.74	87.7
Taxes at 15% investment	6.07	2.43	6.15
ROI at 15% investment	6.07	2.43	6.15
Sales per year	99.00	39.60	100.00
(25 each 100 MWh units)			

Investment:		
Working capital at 30% FC	26.06 MM	
Equipment	14.38 MM	
	40.44 MM	

low rates in positive mixes having only small concentrations of Lewis acidity (molar excess of AlCl$_3$ over NaCl) at top-of-charge, and when the charge cut-off voltage is limited to 3.75 V. Vapor deposited tungsten over the nickel retards this corrosion rate even more. The combination of tungsten coated nickel collectors, control of positive mix composition, and 3.75 V top-of-charge is a promising economic long life solution to the corrosion problem.

Compression seals made originally on the beta alumina tube are now made on alpha alumina flanges glass-sealed to the beta tube. With these seals 20 Wh cells are presently being tested in ambient oven air. Ultimately, however, thermal bonded seals of the anode and cathode compartments must be developed to meet economic, life and energy density goals.

At an estimated price of $39/kWh the Na/SbCl$_3$ battery is above the upper limit of the present U.S. utility load leveling battery target price of $33/kWh for a 5 h battery with a 10 year 2500 cycle life. To reach this goal the operating reliability of seals and the beta alumina solid electrolyte must be significantly improved and produced at lower cost. Competition of the Na/SbCl$_3$ system with the Na/S system is now hampered by the relatively low output of the SbCl$_3$–NaAlCl$_4$–carbon positive mix (0.41 Wh/cm^3) *versus* the sulfur–carbon mix output (1.00 Wh/cm^3) at the same 5 hour rate [4]. Attempts to increase the SbCl$_3$ content of the positive mix and its energy output have been partly successful, but the *insoluble* discharge reaction products (Sb and NaCl) mask the surface of the beta alumina and limit output to a maximum value of 0.5 - 0.6 Wh/cm^3 mix during early cycles. Efforts to increase the solubility of NaCl through complexing agents substituted for some of the AlCl$_3$ in the positive mix are in progress and are promising.

Acknowledgements

References

1 J. Werth, Sodium–chloride battery development program for load leveling, EPRI EM230, Project 109, Interim Report, December 1975.
2 A. M. Chreitzberg, Sodium–antimony trichloride battery development program for load leveling, EPRI EM751, Project 109-3, Interim Report for Period January 1, 1976 - June 30, 1977.
3 J. H. B. George, Proposed criteria for estimating the capital costs of advanced battery systems for utility energy storage, EPRI 787-1, Interim Report, November 1976.
4 I. S. Klein, Sodium–sulfur cell development, Document 7239, March 31, 1978.